Orthogonal electric and ionic conductivities in the thin film of a thiophene-thiophene block copolymer

Yamamoto, Sonoka ; Yamashita, Ryutaro ; Kubota, Chihiro ; Okano, Kentaro ; Kitamura, Masatoshi ; Funahashi, Masahiro ; Ye, Syu-Cheng ;…

(Citation)
Journal of Materials Chemistry C,11(7):2484-2493

(Issue Date)
2023-02-21

(Resource Type)
journal article

(Version)
Accepted Manuscript

(URL)
https://hdl.handle.net/20.500.14094/0100479346

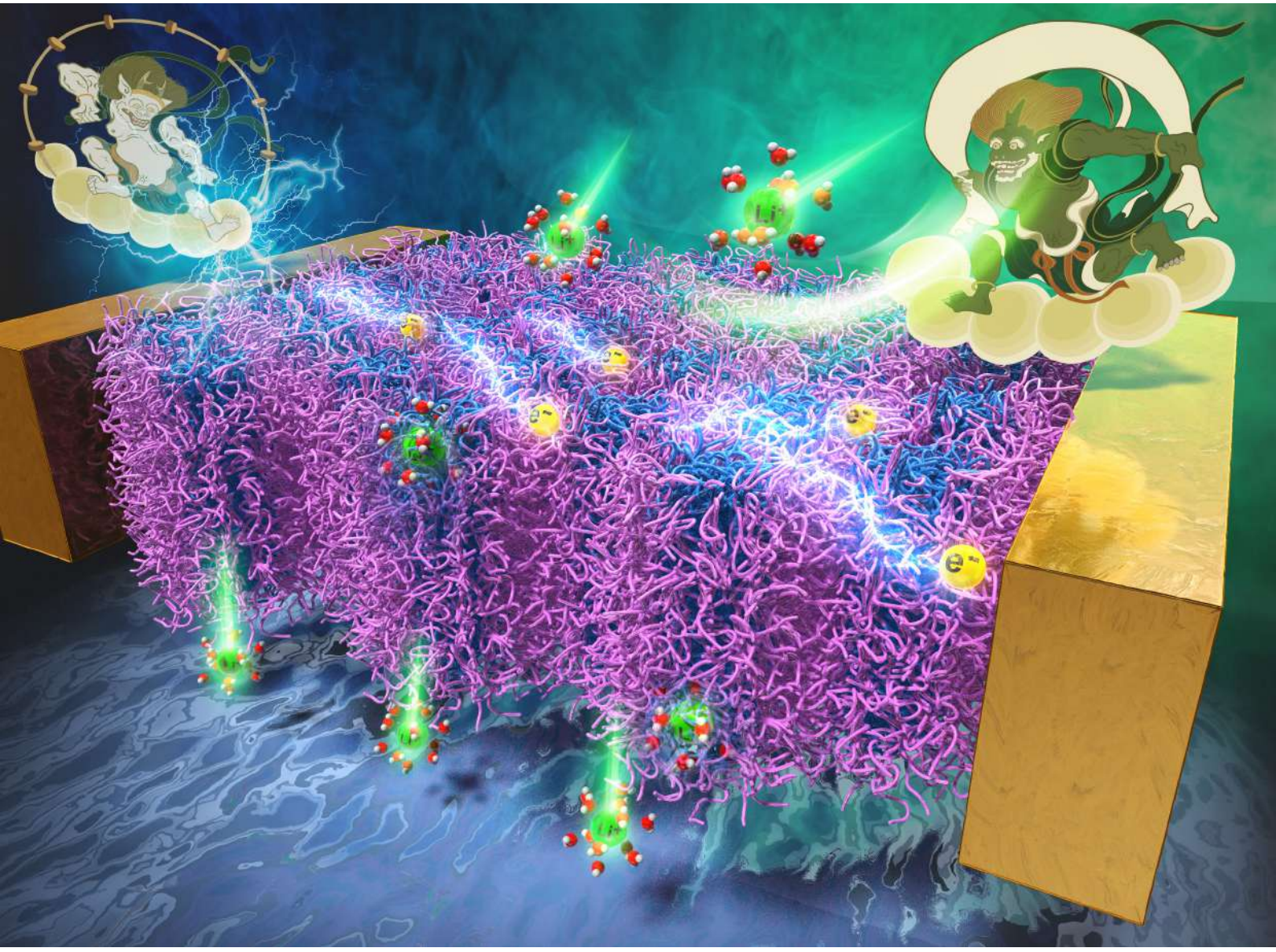
Li+
e-

Paper

Orthogonal electric and ionic conductivities in the thin film of thiophene–thiophene block copolymer

Received 00th January 20xx,
Accepted 00th January 20xx

DOI: 10.1039/x0xx00000x

Sonoka Yamamoto,[a] Ryutaro Yamashita,[a] Chihiro Kubota,[a] Kentaro Okano,[a] Masatoshi Kitamura,[a] Masahiro Funahashi,[b] Syu-Cheng Ye,[c] Yung-Tin Pan,[c] Masaki Horie,[c] Takuji Shintani,[d] Hironori Murata,[a] Hideto Matsuyama,[ad] and Atsunori Mori*[ad]

Thiophene–thiophene block copolymer composed of hydrophilic and hydrophobic side chain functionalities was designed and synthesized. Deprotonative metalation nickel-catalyzed polymerization protocol successfully afforded the block copolymer, which side chains are derived from alkyl and benzenesulfonic acid ester groups. The benzene sulfonate moiety of the block copolymer in the film state was shown to be transformed into the hydrophilic sulfonic acid upon thermal treatment at ca. 200 °C without addition of an external additive. Thus formed block copolymer thin film exhibited cylindrical microphase separation and the hydrophilic domain was revealed to penetrate the film perpendicularly to the substrate. Measurement of electric conductivity suggested that the block copolymer thin film was conductive parallel to the substrate, while the film was insulative to the perpendicular direction. Electrochemical analyses revealed that lithium ion transfers through the cylindrical domain composed of benzene sulfonic acid side chain, which is perpendicular to the substrate. These results represent dual and orthogonal conductivities of electron and ion in the block copolymer thin film.

1. Introduction

Polythiophenes are currently the subject of extensive research attention as electronic materials for conductive and semiconductive devices.[1–3] In particular, regioregular poly(3-substituted thiophene)s, in which the regularity is controlled in a head-to-tail (HT) manner, exhibit particularly suitable electric properties for this purpose. Accordingly, the development of facile synthetic protocols to afford HT-type polythiophenes is a major concern in synthetic chemistry.[4–6]

We have previously reported a deprotonative polythiophene synthesis that involves the reaction of a 2-halo-3-substituted thiophene with magnesium amide to afford the corresponding organometallic monomer,[7–11] which may then be subjected to cross-coupling polymerization followed by the addition of a nickel catalyst to afford a regioregular HT-type polythiophene with a well-controlled molecular weight as shown in Figure 1a.

Furthermore, the rational design and introduction of side-chain moieties can be employed to confer additional functionality to polythiophenes.[12–14] For instance, we have previously reported that (i) the introduction of an oligosiloxane side-chain moiety improves the solubility of the polythiophene in organic solvents, particularly hydrocarbons such as hexanes;[15] and (ii) polythiophenes bearing benzenesulfonic acid ester groups undergo thermally-induced doping of the polymer main chain upon the thermal decomposition of neopentyl benzene sulfonate to the corresponding sulfonic acid. This transformation at the side chain allows doping of the polythiophene main chain while simultaneously conferring water-solubility to the polymer. (Figure 1b)

Our extensive researches into the structural design of polythiophenes have focused on the introduction of composite functionality, which can be achieved by the synthesis of polythiophene copolymers comprising monomers with different functional groups on their side chains.[16,17] For instance, we have recently reported that introducing a small amount of a thiophene comonomer with thermally-induced-doping functionality to poly(3-alkylthiophene) imparts self-doping ability to the resultant random copolymer.[18]

Our further concern is turned to the synthesis of copolymers composed of different polythiophene moieties, which represents a breakthrough in terms of functionality design in polythiophene synthesis.[19] Because formation of a block copolymer induces microphase separation in its corresponding polymer film, such films have application potential in areas such as selective gas permeation, ion transfer, etc.[20] It has been shown that a block copolymer with a certain ratio of each copolymer exhibits microdomain structure as cylinder or lamellar. Therefore, such a microphase separation would form penetrating substructure in the thin film state on a substrate.[21–23] Specifically, a copolymer containing some

[a] Graduate School of Engineering, Kobe University, 1-1 Rokkodai, Nada, Kobe 657-8501, Japan. Email: amori@kobe-u.ac.jp
[b] Department of Advanced Materials Science, Kagawa University, 2217-20 Hayashi-cho, Takamatsu, Kagawa 761-0396, Japan.
[c] Department of Chemical Engineering, National Tsing Hua University, 101, Sec. 2, Kuang-Fu Road, Hsinchu 30013, Taiwan
[d] Research Center for Membrane and Film Technology, Kobe University, 1-1 Rokkodai, Nada 657-8501, Japan

Electronic Supplementary Information (ESI) available: Experimental details, further details on microscopic analyses, SAXS analyses, electric conductivity measurements, and electrochemical analyses. See DOI: 10.1039/x0xx00000x

polythiophene units with benzenesulfonic acid side-chain functionality could potentially form micro-sized domains capable of ion conduction[24,25] along with the electron-conductive characteristics of the overall polythiophene itself. The ion conductivity imparted by discrete sulfonate microdomains would occur in the thin film formed on the substrate.[26,27] However, such characteristics are rarely found in other electronic materials.

Herein, we report the block copolymerization of different types of thiophene monomers with either alkyl or benzenesulfonate side chains. Thin film formed from this copolymer was demonstrated to exhibit cylindrical microphase separation that penetrates throughout the film providing ion conductivity as well as the electrically conductive characteristics of regioregular poly(3-substituted thiophene). Both conductivities of the film are shown to manifest in orthogonal directions perpendicular and parallel to the substrate, respectively. (Figure 1c)

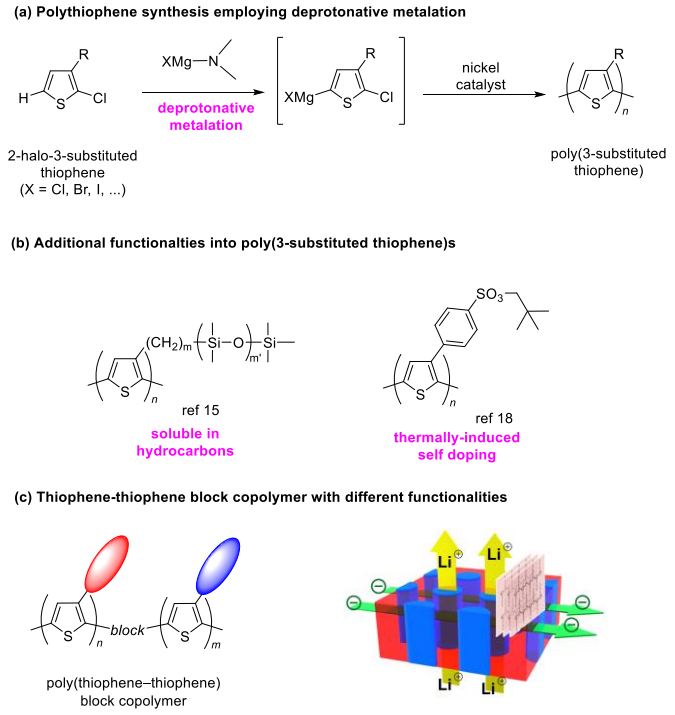

Fig. 1 Synthesis of head-to-tail (HT) type polythiophene and side chain functionality of polythiophenes

2. Results and Discussion

2.1 Synthesis and Characterization

Synthesis of thiophene block copolymer derived from alkyl-substituted **1** and benzenesulfonate **2** was performed as shown in Scheme 1. Initial polymerization of 2-chloro-3-hexylthiophene (**1**) was carried out by reaction with the bulky magnesium amide **3**[28] followed by addition of the nickel catalyst $NiCl_2(IPr)PPh_3$ (**4**) (2 mol% relative to **1**).[7] The second organometallic monomer, which was prepared by the reaction of **2** and magnesium amide **3**, was then added to the polymerization solution.[29] Further stirring of the mixture for 24 h at room temperature afforded block copolymer **5a** in 74% yield. ^{1}H NMR analysis indicated a block ratio of 1.0:0.9 based on the integral values of the methylene signal for the hexylthiophene moiety derived from **1** $(2H)_n$ and the neopentyl methylene signal from **2** $(2H)_m$.

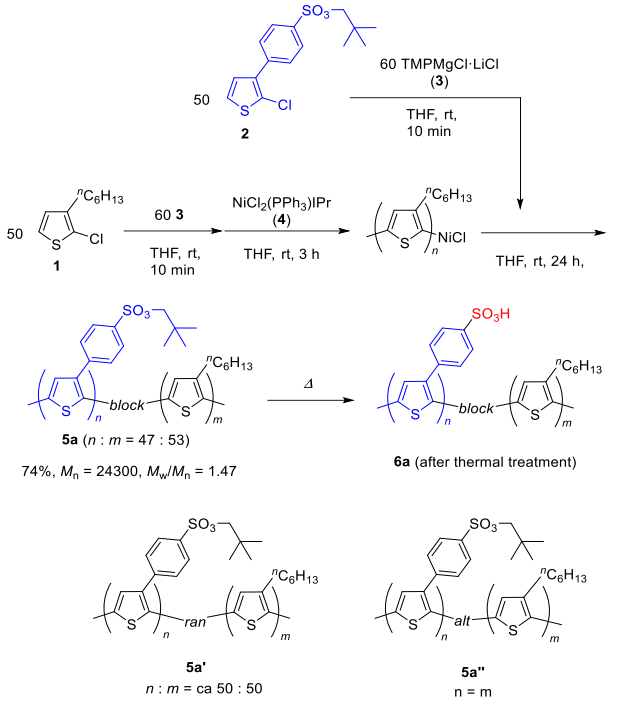

Scheme 1 Synthesis of head-to-tail (HT) type polythiophene and side chain functionality of polythiophenes

Block copolymerization of monomer precursors **1** and **2** at different ratios was also performed. Table 1 shows the details of these products. The reactions provided the corresponding products in good to excellent yields with reasonable average molecular weights (M_n) and relatively narrow molecular weight distributions (M_w/M_n). The ratios of the components in block copolymers **5b–g** were estimated from their ^{1}H NMR spectra and are presented as *n*:*m*. This ratio was found to correspond reasonably well with the feed ratio of the monomer precursors **1** and **2**. These results show that polymerization of metalated **2** proceeds at the living end of the polymerized alkylthiophene **1** smoothly and revealed that incorporation of both metalated monomers of **1** and **2** took place at room temperature within 24 h.

Table 1 Characterization of block copolymers **5** with different feed ratios[a]

5	1/2[a]	Yield (%)	M_n (M_w/M_n)[a]	*m*:*n*[b]
5a	0.5:0.5	74	24300 (1.47)	0.53:0.47 (62%)
5b	0.8:0.2	71	16000 (1.73)	0.83:0.16 (28%)
5c	0.7:0.3	87	13000 (1.75)	0.76:0.24 (37%)
5d	0.6:0.4	79	17700 (1.62)	0.67:0.33(48%)
5e	0.4:0.6	83	24000 (1.36)	0.43:0.57(71%)
5f	0.3:0.7	71	21800 (1.32)	0.29:0.71 (82%)
5g	0.2:0.80	48	14000 (1.32)	0.21:0.79 (87%)

[a] The first polymerization was carried out by the reaction of chlorothiophene **1** (0.3 mmol), TMPMgCl·LiCl (3, 0.33 mmol) and nickel catalyst **4** in THF. Polymerization was carried out for at room temperature 3 h. The monomer derived from **2** (0.3 mmol) was added to the reaction mixture for the first polymerization to initiate the second propagation and the resulting thiophene-thiophene block copolymer 5 was obtained as a dark purple solid. [b] The feed ratio of **1** and **2** (mol/mol). In parenthesis, mass ratio of the benzenesulfonate moiety was shown. [c] M_n and M_w/M_n were determined by SEC analysis based on polystyrene standards. [d] The ratio of *m*:*n* was determined by ^{1}H NMR analysis.

The obtained copolymer **5a** was found to be soluble in organic solvents such as chloroform and THF. However, it was found to be insoluble in both chloroform and water after being heated at ca. 200 °C for 10 min. This result indicates the formation of an amphiphilic block copolymer **6a** bearing hydrophobic alkyl groups and hydrophilic sulfonic acid (–SO_3H) pendant groups. It is very different from the result for the corresponding benzenesulfonate-bearing homopolymer, which is soluble in water after heating. We also prepared and characterized two related copolymers, both with a similar *n*:*m* ratio to that of **5a**. These were the random **5a'** by copolymerization of **1** and **2**[18] and the alternating copolymer **5a''**, which was prepared by the polymerization of a bithiophene dimer bearing both the substituents present on **1** and **2**[16].

The TG-DTA trace for **5a** (*m*:*n* = ca. 0.5:0.5) shows a weight loss of ca. 15% at 200 °C. (Figure 2) This result was found to agree reasonably with the calculated ^{1}H NMR result (*m*:*n* = 0.53:0.47) and the molecular formulas of **2** –$(C_{10}H_{14}S)_m$–$(C_{15}H_{16}S_2O_3)_n$–, indicating a 14% loss under the elimination of C_5H_{10} from the side-chain neopentyl sulfonate. Based on the results from TG-DTA, spectroscopic analyses of block copolymer **5a** in the film state were performed on a quartz substrate. Measurements after thermal treatment were performed by heating the substrate at 200 °C for 20 min. As shown in Figure 3a, the UV–Vis absorption spectrum of **5a** in the film state shows a λ_{max} value of ca. 560 nm, while an emergent absorption at >700 nm along with a decrease in absorbance at λ_{max} is observed in **6a** upon thermal treatment, suggesting that thermally-induced self-doping of the polythiophene main chain via the formation of SO_3H on the side chains occurs.[18] We next measured XRD with the thin film of block copolymer **6a** after thermal treatment. The measurement of the out-of-plane profile revealed that a characteristic peak at 2θ = 5.4°, which was assigned as (100) reflection suggesting layer distance derived from polythiophene side chain (16.4 Å). In contrast, a peak at 2θ = 15°–20° that was characterized as layer distance between conjugated polymers with with with π–π satcking (5.7 Å) was broad and relatively smaller toward (100) reflection. (Figure 3b) These results in the out-of-plane measurement strongly suggest edge-on preference of the polythiophene film on the substrate whereas attempted in-plane measurement was unsuccessful.

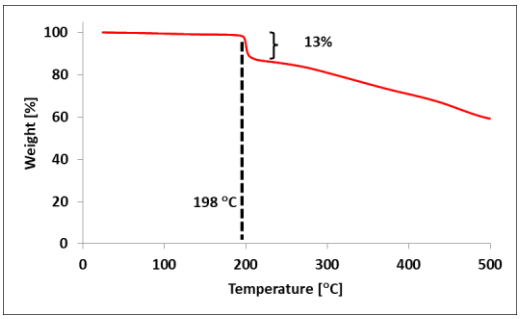

Fig. 2 TG-DTA profile of block copolymer **5a**

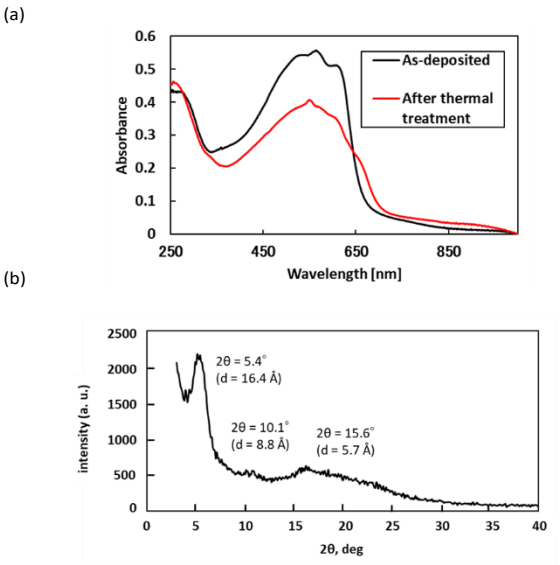

Fig. 3. (a) UV-vis absorption spectra of block copolymer **5a** before and after thermal treatment. (b) X-ray diffraction pattern (out-of-plane) of **5a** after thermal treatment on a glass substrate.

2.2 Microscopic analyses of block copolymer thin films

We next investigated the properties of **5a** as a thin film. Copolymer films were fabricated by spin coating a chloroform solution of **5a** (ca. 5 mg/mL) on a glass substrate. The spin-coated thin film was formed at a spin rate of 1000 rpm for 1 min. The obtained thin films were heated at 200 °C for 20 min, and AFM observation was performed before and after thermal treatment.[24] Block copolymer **6a** exhibits a clear dotted pattern in the tapping mode after heating, indicating

microphase separation. The dark images suggests the polythiophene domain bearing benzene sulfonic acid moiety at the side chain, while the bright ones as the alkylthiophene domain. Such a phase separation is only observed in the thermally-treated film, whereas significant phase separation is not observed clearly for the as-cast film. In addition, this microphase separation is not observed despite after heating for the random copolymer **6a'** or the alternating copolymer **6a''** (Figure 4a–d).

These results suggest that microphase separation appears in **6a** after thermal treatment at 200 °C for 20 min owing to the presence of the two different side chains in a specific arrangement. Although the dotted pattern is not observed for **5a** before heating, this does not necessarily show that phase separation proceeds upon heating of the as deposited film, because it becomes much more apparent in AFM observation after the decrease in volume caused by the elimination of the neopentyl group (as C_5H_{10}). Considering that the related dotted pattern was not observed in the related random (**6a'**) or alternating (**6a''**) copolymer (Figure 4c, 4d, respectively), these results also support that the observed dots are the resultant of microphase separation and the formation of a gas bubble by the evolving C_5H_{10} may also be ruled out. (See also Figure S1 and S2)

Similar to the results for AFM, the TEM image of **6a** (Figure 4e) was measured at 200 kV and shows a dotted pattern, albeit weak contrast because of the structural similarity of the main chain in each domain, as that observed by AFM,[23,30–32] confirming that the thin film of **5a** features cylindrical phase separation that penetrates the film perpendicularly to the substrate. Measurement of small-angle X-ray scattering (SAXS) of **6a** also supported the formation of the microphase separation. As shown in Figure 4f, the SAXS curve showed a primary peak along with a hump. The interdomain distance D determined from the peak position was 28.46 nm, which agreed with that estimated by AFM and TEM analyses. It should be noted that such a peak was only observed in the thermally-treated block copolymer, which no peak was found in **5a** before thermal treatment as well as the corresponding random copolymer **5a'**. (See also Supporting Information)

We also subjected **5b**–**5g** to AMF analysis, as shown in Figure 4g. Similar dotted patterns are observed for **6b**, **6c**, **6d**, and **6e** but not for **6f** and **6g**. This suggests that phase separation occurs after heating when the alkylthiophene moiety content is high, while a higher benzenesulfonate content appears to disrupt the phase separation.

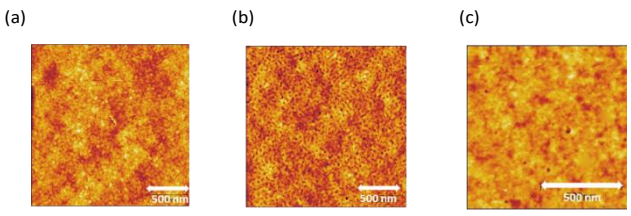

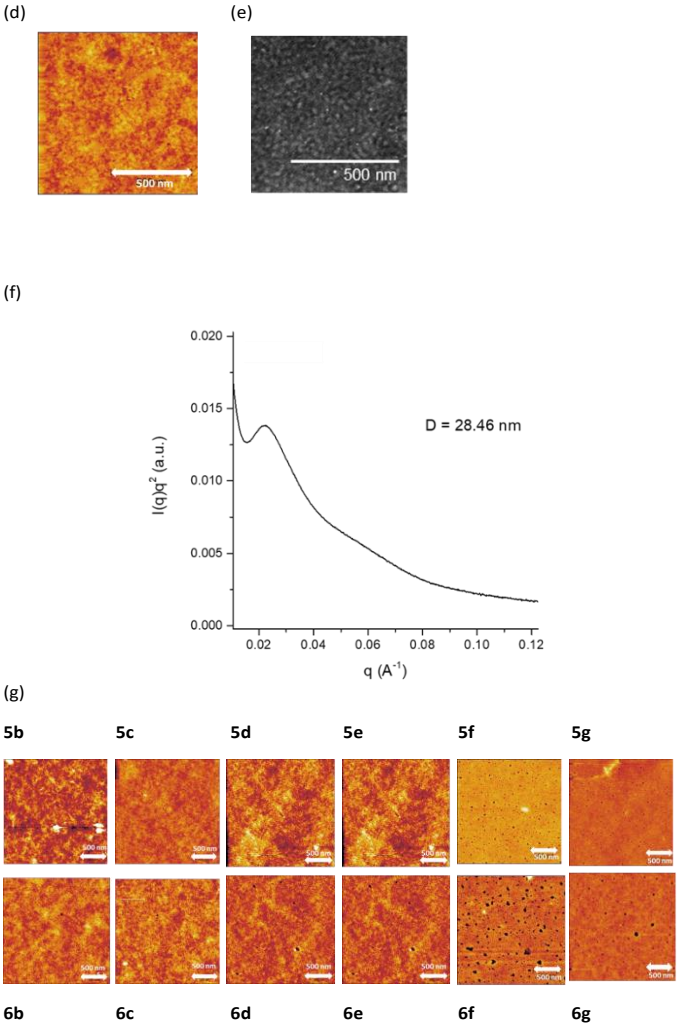

Fig. 4. AFM and TEM images of copolymers **5** derived from **1** and **2** moieties. (a) AFM image of block copolymer **5a** before thermal treatment. (b) block copolymer **5a** after thermal treatment. (c) random copolymer **5a'** after thermal treatment (d) alternating copolymer **5a''** after thermal treatment (e) TEM image of block copolymer **5a** at 200 kV after thermal treatment. (f) SAXS profile of block copolymer **5a** after thermal treatment. (g) AFM images of block copolymers with different ratio of alkyl and benzenesulfonate substituents before (**5b**-**g**) and after the thermal treatment (**6b**-**g**).

2.3 Electric properties of thin films

Having confirmed the potential occurrence of cylindrical microphase separation that penetrates the thin film, we next studied the electric properties of the films of block copolymers **5**, which were fabricated on ITO electrodes or glass substrates, where gold electrodes were deposited as shown in Figure 5. The ITO electrode was deposited on a quartz substrate with a gap length of ca. 200–800 μm and a chloroform solution of the block copolymer was cast on the electrode, and the thickness of the film was found to be ca. 200 nm, as depicted in Figure 5a.[33] Conductivity measurements toward the parallel direction on the substrate were performed in the applied voltage range 0–100 V.

The conductivity toward the perpendicular direction to the substrate was measured with the gold electrode at a lower voltage (0–10 V) as shown in Figure 5b, with a gap length of ca.

80 µm and film thickness of ca. 200 nm, where the film was cast on the Au electrode followed by the additional deposition of Au electrode on the polythiophene film. The related gold electrode for the measurement of parallel direction under similar conditions to Figure 5b (0–10 V) was also applied as shown in Figure 5c, which widths of the Au electrodes were set as 1.4 mm and 100 µm, respectively, and the film thickness was 200 nm.

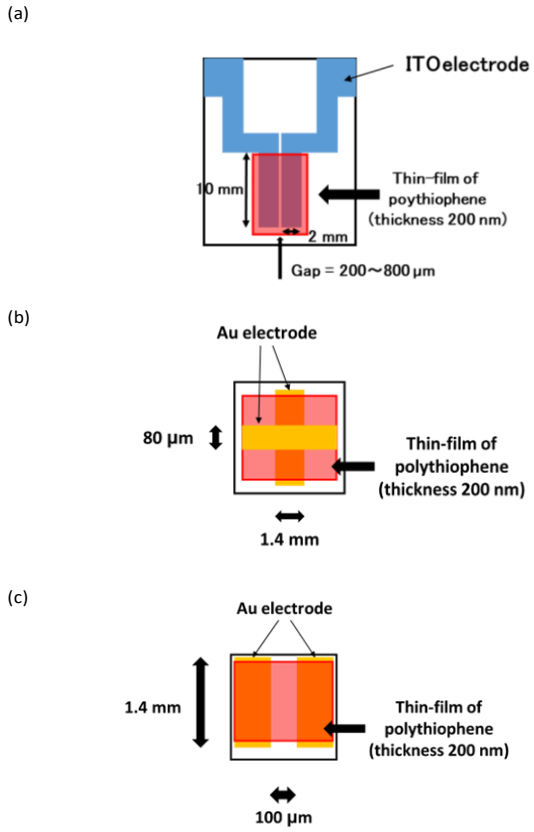

Fig. 5. Measurement of electric conductivity of block copolymer thin film of **5**. (a) Measurement of the conductivity of the thin film of block copolymer **5** before/after thermal treatment at the applied voltage up to 100 V. (b) at low voltages (0–10 V) perpendicular to the film on the substrate. (c) at the low voltage parallel to the film (0–10 V) .

The conductivities of the block copolymers at an applied voltage of 100 V before and after thermal treatment are summarized in Table 2. It was found to show the conductivities of **5a** is 8.92×10^{-5} S/cm before thermal treatment and **6a** 9.37×10^{-3} S/cm (100 V) after. This suggests that the conductivity is improved ca. 100-fold by thermal treatment. A smaller improvement in conductivity is observed for copolymer **6b** because of its lower benzenesulfonate content (< 20%). Improved conductivity after thermal treatment is observed for **6g** owing to its higher sulfonate content, albeit with little microphase separation. The conductivity after thermal treatment is observed toward the parallel direction on the substrate. The results suggest that the polythiophene block copolymers **5** in the film state on the substrate is cast as edge-on orientation as depicted in Figure 1c (right).

It should be pointed out that measurement of the conductivity with the thin film of Figure 5b at the applied voltage of 0–10 V is remarkably low even after thermal treatment showing insulative characteristics to the perpendicular direction. On the other hand, the related Au electrode (Figure 5c) showed the much superior conductivity of **6a** (1.58×10^{-3} S/cm at 10 V) to the parallel direction of the film similar to the case of the ITO electrode. These results support the edge-on orientation of the thiophene–thiophene block copolymer **5a** and that the thermally-induced self doping of the polythiophene moiety bearing benzenesulfonic acid affected the improved conductivity to the poly(alkylthiophene) moiety.[34,35]

Table 2. Summary of the results of the electric conductivity of polythiophene block copolymers **5a**[a]

	1/2 (mol/mol)[b]	Applied voltate, V[c]	Conductivity before thermal treatment, Scm^{-1}	Conductivity after thermal treatment, Scm^{-1}
5a	0.53/0.47	100 (a)	8.92×10^{-5}	9.37×10^{-3}
5b	0.83/0.16	100 (a)	1.10×10^{-5}	2.51×10^{-4}
5g	0.21/0.79	100 (a)		8.12×10^{-2}
5a	0.53/0.47	10 (b)		6.06×10^{-10}
5a	0.53/0.47	10 (c)	1.75×10^{-4}	1.58×10^{-3}

[a] Measurements were carried out using devices as depicted in Figure 5 (a)–(c). [b] The ratio derived from **1** and **2** in the block copolymer of **5**. Based on the result of 1H NMR measurement. [c] In parenthesis, the measured device in Figure 5 was shown.

2.4 Electrochemical properties of thin films

We then measured the ionic conductivities of **5a** and **5a'** by electrochemical impedance spectroscopy (EIS) using a conventional three-electrode setup in an aqueous solution of 0.5 M Li_2SO_4, as shown in Figure 6a.[36] The working electrode, composed of the polymer thin film spin coated onto ITO glass, and the Pt reference electrode were configured such that the measurements reflect through-plane charge transport.

The Nyquist plot acquired for the thermally-treated film of **6a** at 0.6 V vs. reversible hydrogen electrode (RHE) features an additional semicircle at the high-frequency region, as shown in Figure 6b (red plot), while that of **6a'** does not (black plot). The plots for **6a** and **6a'** can be fitted with an equivalent circuit composed of one resistor (R_s) in series with two resistor–capacitor (R_1-CPE_1 and R_2-CPE_2) units (Figure 6b, solid lines). The impedances and capacitances of the systems fabricated with **6a** and **6a'** were estimated as summarized in Table 3, demonstrating the remarkably low R_1 and R_2 values for **6a** compared with those for**6a'**. The obtained values for resistance for **6a**, both R_1 and R_2, were 2.06×10^2 W·cm^2 and 8.06×10^4 W·cm^2, respectively. These values were significantly lower than those obtained for **6a'**, which were 3.48×10^4 W·cm^2 and 2.66×10^5 W·cm^2 respectively (Table 3).

Table 3 Summary of EIS equivalent circuit fitting[a]

	R_1[b] (Ω cm²)	CPE[b] (F/cm²)	R_2[c] (Ω cm²)	CPE_2-T[c] (F/cm²)
5a	2.06×10^2	9.67×10^{-5}	8.06×10^4	7.38×10^{-5}
5a'	3.48×10^4	9.04×10^{-5}	2.66×10^5	2.03×10^{-5}

[a] The measurement was performed as illustrated in Figure 6(a). [b] Impedance and capacitance of copolymer before thermal treatment. [c] Impedance and capacitance of copolymer after thermal treatment.

Cyclic voltammetry (CV) analysis of **5a** and **6a** (Figure 6c) supports the EIS results. A cyclic voltammogram is only clearly observed for the thermally-treated film of **6a**, and the capacitance was calculated to be 0.431 $mFcm^{-2}$ at a scan rate of 200 mVs^{-1}, as compared with 0.08 $mFcm^{-2}$ before thermal treatment. In addition, the excellent retention of capacitance compared with that at the slower scan rate of 20 mVs^{-1} (21% loss) reflects the superior ionic conductivity of thermally treated **6a**. The cyclic voltammograms for **5a'** and **6a'** also show differences before and after thermal treatment, but the capacitance of **5a'** is much lower (Figure 6d). Furthermore, even after thermal treatment, **6a'** loses 71% of its capacitance when the scan rate is increased from 20 to 200 mVs^{-1}.

These results show that lithium-ion conductivity is observed for the thermally-treated copolymers **6a** and **6a'**, while the as-cast films are much less ion conductive. Because thermal treatment of the polythiophene film converts benzenesulfonate ($–SO_2OR$) into the corresponding sulfonic acid ($–SO_3H$), lithium ions can interact with the SO_3^- moiety, resulting in ion conductivity.

Compared with the corresponding values for **6a'**, the lower resistance of **6a** by EIS measurements as well as its higher capacitance and smaller decrease upon increasing the CV scan rate (200 vs. 20 mVs^{-1}) indicate that **6a** does indeed feature channel domains that transport hydrated lithium ions, as depicted in Figure 6e. These results also correspond with the AFM and TEM results shown in Figure 4, which support the formation of cylinder-like microphase separation regions penetrating the film perpendicular to the substrate.

Combined with the electric conductivity measurements shown in Figure 5, the thin film of **6a** exhibits *dual orthogonal conductivities for electrons (parallel to the substrate) and lithium ions (perpendicular to the substrate)*. To the best of our knowledge, these unique characteristics have not been observed in any previous polythiophene materials.

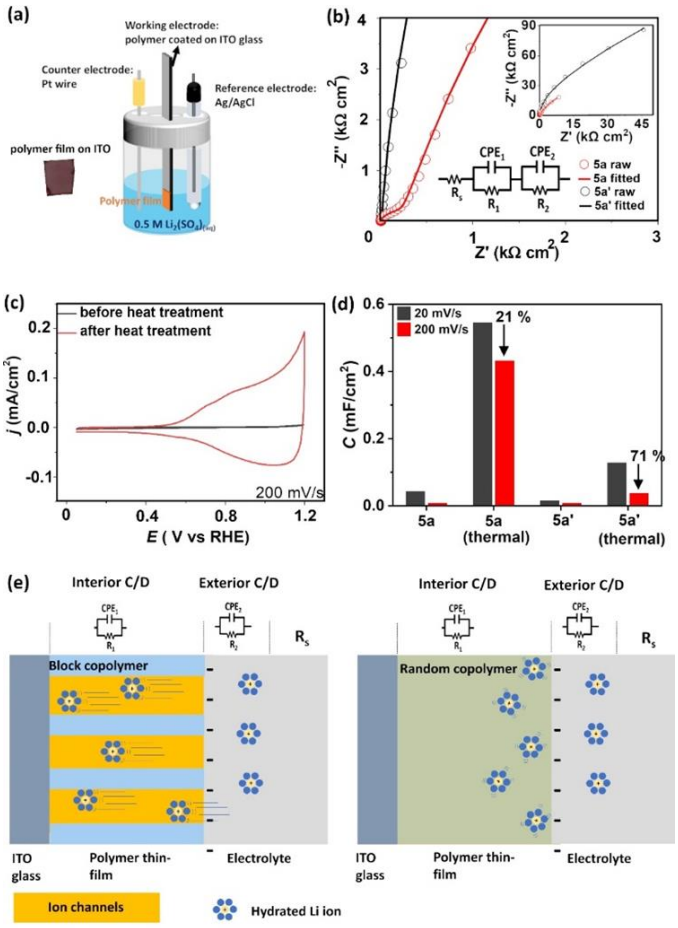

Fig. 6. Measurements of EIS and CV. (a) Measurements of EIS and CV with three electrode electrochemical setup. (b) Nyquist plots of heat treated films of **5a** and **5a'** (inset: at lower frequency and a EIS model). (c) CVs of a film of 5a before and after heat treatment. (d) Results of the measured capacitance of **5a** and **5a'** before and after heat treatment. (e) Schematic illustration of the transfer of hydrated lithium ion through the copolymers **5a** and **5a'**.

3. Conclusions

We have demonstrated the novel properties of thiophene–thiophene block copolymers containing hydrophobic and hydrophilic side-chain structures. By employing block copolymerization of alkylthiophene **1** and benzenesulfonate pendant thiophene **2** followed by thermal treatment of the sulfonate ester leading to the corresponding sulfonic acid, a new class of amphiphilic block copolymers bearing hydrophilic and hydrophobic moieties composed of single polythiophene main chain was produced. Such block copolymers undergo microphase separation, as confirmed by AFM and TEM analyses. Electric conductivity measurements showed that, after thermal treatment, electrons transfer parallel to the thin-film substrate and that the film is insulative in the perpendicular direction based on the edge-on orientation of polythiophene. Conversely, lithium-ion channels through the domain of polythiophene bearing sulfonic acid at the side

chain are formed perpendicular to the substrate. Thus, orthogonal dual functionality in terms of electron and ion transportation have been achieved in polythiophene–polythiophene block copolymer thin films.

4. Experimental Section

4.1 General

All the polymerization procedures were performed in the glove box under an argon atmosphere or standard Schlenk technique under nitrogen. ^{1}H NMR (400 MHz) and ^{13}C{^{1}H} NMR (100 MHz) spectra were measured on JEOL ECZ400 as a $CDCl_3$ solution unless noted. The chemical shifts were expressed in ppm with $CHCl_3$ (7.26 ppm for ^{1}H) or $CDCl_3$ (77.00 ppm for ^{13}C) as internal standards. SEC (size exclusion chromatography) analyses were performed with a standard HPLC system equipped with UV detector at 40 °C using chloroform as an eluent with a Shodex GPC KH-404HQ or the related column. Molecular weights and molecular weight distributions were estimated on the basis of the calibration curve obtained by 6 standard polystyrenes (M_n = 2630-355000). High resolution mass spectra (HRMS) were measured by JEOL JMS-T100LP AccuTOF LC-Plus (ESI) with a JEOL MS-5414DART attachment. Elemental analyses were carried out at the Department of Instrumental Analysis & Cryogenics Division of Instrumental Analysis, Okayama University on a Perkin–Elmer 2400II Elemental analyzer supported by Inter-University Network for Common Utilization of Research Equipments. IR spectra were recorded on Bruker Alpha with an ATR attachment (Ge). UV-vis spectra (as a thin film) were measured with a Shimadzu UV-3101PC. Thermal analyses were carried out with RIGAKU Thermo plus EVO2 TG-DTA 8121. XRD analysis was carried out with Rigaku SmartLab with the power of 40 kV, 30 mA, and the wavelength of 1.5418 Å (CuKα). The incidence angle α of the X-ray beam was 0.20°. The XRD measurements were performed with the out-of-plane geometry. Measurements of Atomic Force Microscope (AFM) of the thin film were performed as a tapping mode by Shimadzu UV-3101PC. Measurement of TEM was performed by HITACHI-SU8010 (200 kV). The formation of polymer thin films was performed with spin coater SWINCO and the thickness of the film was measured with stylus profiler ULVAC DEKTAK8. SAXS measurements (transmission mode) were conducted at beamline TPS13A of the National Synchrotron Radiation Research Center (NSRRC), Hsinchu, Taiwan. The energy of the employed monochromatic radiation was 15 keV, prescribing the X-ray wavelength λ of 0.8266 Å. The 2D scattering patterns were collected with an In-vacuum Eiger X 9M(SAXS) detector. The conductivity of polymer films was measured with a digital electrometer ADCMT8340A and Agilent B1500 semiconductor parameter analyzer. Measurement of cyclic voltammetry and electrochemical impedance spectroscopy (EIS) analysis was carried out with a Biologic SP-200 potentiostat. For thin layer chromatography (TLC) analyses throughout the work, Merck precoated TLC plates (silica gel 60 F_{254}) were used. Purification by HPLC with preparative SEC column (JAI-GEL-1H, JAI-GEL-2H) was performed by JAI LC-9201.

4.2 Materials

Thiophene derivatives bearing a substituent at the 3-position was prepared in a manner shown in the literatures. Chlorination of 3-hexylthiophene (**1**) was carried out in a similar manner as reported previously.[7] Chlorothiophene bearing a benzenesulfonate group at the 3-position 2-chloro-3-(4-(2,2-dimethylpropylsulfonylbenzne)-1-yl)thiophene (**2**) was synthesized in a manner as reported.[16] Magnesium amide (TMPMgCl·LiCl 2,2,6,6-teteramethylpiperidine-1-yl chloromagnesium lithium chloride salt (**3**): Knochel–Hauser base[37]) was purchased from Sigma-Aldrich Co. Ltd. as a 1 M THF solution. Nickel catalyst $NiCl_2$(IPr)PPh_3 (**4**, IPr: 1,3-bis(2,6-diisopropylphenyl)imidazolin-1-yl)[38] was purchased from TCI Co. Ltd. and employed as a catalyst for the polymerization as received. Random copolymer poly[(3-hexylthiophen-2,5-diyl)$_m$-*ran*-(3-(4-(2,2-dimethylpropylsulfonylbenzne)-1-yl)thiophen-2,5-diyl)$_n$] (**5a'**, m:n=ca. 1:1) was prepared in a manner as we reported previously.[18] THF (anhydrous grade) was purchased from Kanto Chemical. Co. Ltd. and passed through alumina and copper column (Nikko Hansen & Co. Ltd.) or distilled from sodium dispersion in a mineral oil/benzophenone ketyl prior to use.[39]

4.3 Synthesis of diblock copolymers

poly[(3-hexylthiophen-2,5-diyl)$_m$-*b*-(3-(4-(2,2-dimethylpropylsulfonylbenzn)-1-yl)thiophen-2,5-diyl)$_n$] (**5a**): To a screw-capped test tube equipped with a magnetic stirring bar were added 2-chloro-3-hexylthiophene (**1**, 0.66 mL, 0.3 mmol) and THF (3 mL) in a glove box. A 1 M THF solution of TMPMgCl·LiCl (**3**, 0.36 mL, 0.36 mmol) was added to the resulting mixture and stirring was continued for 10 min to form the corresponding organometallic monomer. Nickel catalyst $NiCl_2$(IPr)PPh_3 (**4**, 4.7 mg, 6 x 10^{-6} mol) was added to the THF solution of the monomer and the mixture was stirred for 3 h to initiate the polymerization. Chlorothiophene bearing a benzenesulfonate group **2** was dissolved in 3 mL of THF in a screw-capped test tube equipped with a magnetic stirring bar. Magnesium amide **3** was added to the solution and stirring was continued for 10 min at room temperature. The resulting solution was added to the solution of the living polymer derived from **1** and the mixture was removed from the glove box and stirring was further continued for 24 h at room temperature. The reaction was terminated by the addition of 1 M hydrochloric acid to form a dark purple precipitate, which was filtered off and washed repeatedly with methanol and diethyl ether to afford the block copolymer **5a** (106 mg, 74%). The average molecular weight and the PDI value was estimated by SEC analysis to reveal M_n = 24300; PDI = 1.47. The ratio of the each block was calculated by ^{1}H NMR measurement (*m*:*n* = 1.0:0.9). ^{1}H NMR (400 MHz, $CDCl_3$): δ 7.89 (d, 2H, *J* = 8.2 Hz), 7.55 (d, 2H, *J* = 8.2 Hz), 6.98 (s, 1H), 6.93 (s, 1H), 3.71 (s, 2H), 2.80 (t, 2H, *J* = 7.8 Hz), 1.74–1.67 (br, 2H), 1.44–1.42 (br, 2H), 1.37–1.34 (br, 4H), 0.93–0.84(br, 12H). ^{13}C{^{1}H} NMR (100 MHz, $CDCl_3$) δ 140.0, 137.9, 135.6, 134.1,

133.8, 130.1, 128.7, 128.4, 80.0, 31.8, 30.6, 29.5, 29.4, 26.1, 22.7 14.3. Several signals were found to be not observed because of their broadening. IR (ATR) 3760, 3483, 3409, 2971, 2958, 1739, 1366, 1228, 1217, 1188 cm^{-1}.

The related block copolymers **5b**-**5g** composed of different ratio of *m*:*n* were prepared in a similar manner shown above and the results are summarized in Table 1.

4.4 Synthesis of 2-Chloro-5-(3-hexylthiophen-2-yl)-3-(4-(2,2-dimethylpropylsulfonylbenzen)-1-yl)thiophene

Preparation of such bithiophene was carried out in a manner as reported previously.[16] (52% yield) ^{1}H NMR (400 MHz, $CDCl_3$): δ 7.88 (d, 2H, *J* = 8.2 Hz), 7.54 (d, 2H, *J* = 8.2 Hz), 7.33 (d, 1H, *J* = 5.0 Hz), 7.09 (d, 1H, *J* = 5.0 Hz), 6.70 (s, 1H), 3.71 (s, 2H), 2.49 (t, 2H, *J* = 7.8 Hz), 1.47–1.57 (m, 2H), 1.26–1.36 (m, 6H), 0.91 (s, 9H); ^{13}C {^{1}H} NMR (100 MHz, $CDCl_3$): δ 141.7, 140.0, 137.0, 134.8, 132.8, 131.3, 130.1, 130.0, 128.2, 127.9, 125.44, 125.35, 80.0, 31.8, 31.7, 29.6, 29.0, 28.0, 26.2, 22.7, 14.3. IR (ATR) 2960, 2924, 2855, 1597, 1462, 1400, 1362, 1210, 1191, 1178, 974, 937, 836, 756 cm^{-1}. HRMS (DART–ESI$^+$) m/z: calcd for $C_{25}H_{31}{}^{35}Cl^{23}NaO_3S_3$, 533.1021: found, 533.1043.

4.5 Formal synthesis of alternating copolymer 5a''

Synthesis of **5a''** was synthesiszed by the polymerization of bithiophene prepared above in a manner as we have shown previously. (83% yield) ^{1}H NMR (400 MHz, $CDCl_3$) : δ 7.90 (d, 2H, *J* = 8.2 Hz), 7.61 (d, 1H, *J* = 8.2 Hz), 7.01 (s, 1H), 6.85 (s, 1H), 3.71 (s, 2H), 2.74 (brt, 2H, *J* = 7.4 Hz), 1.58–1.68 (m, 2H), 1.25–1.42 (m, 4H), 0.88 (m, 12H); ^{13}C{^{1}H} NMR (100 MHz, $CDCl_3$): δ 141.4, 140.9, 137.2, 135.1, 135.0, 133.0, 132.6, 130.9, 130.3, 130.1, 128.6, 128.3, 79.9, 31.8, 31.7, 30.6, 29.5, 29.3, 26.2, 22.8, 14.3. IR (ATR) 3744, 3649, 3525, 2918, 1357, 1178, 965, 857, 825, 673, 660, cm^{-1}.

4.6 Observation of AFM and TEM images

Polythiophene block copolymer **5**, the related random copolymer **5a'**, and alternating copolymer **5a''** (10 mg, respectively) were dissolved in 0.5 mL of chloroform and cast on a glass substrate and subjected to the measurement. AFM images of polythiophene block copolymer after thermal treatment were observed after thus prepared glass substrate was treated at 200 °C for 20 min. For the observation of the TEM images of block copolymer **5a**, 3 mg of the polymer was dissolved in 450 μL of chloroform and filtered using a 0.45 μm PTFE filter. A 50 μL of the solution was spin-coated on a glass substrate at 100 rpm for 1 min. After annealing at 200 °C for 20 min in air, the film of **6a** was transferred to a TEM grid in a HF aqueous solution and dried in vacuum.

4.7 SAXS measurement of block copolymer 5a

Polymer solid **5a** (4 mg) was dissolved in 0.4 mL of chloroform and the solution was casted on a glass substrate. After removal of the solvent, annealing was performed at 200 °C for 20 min. The polymer film was scratched from the glass substrate by a stainless steel scraper. The measured magnitude of the scattering vector *q* ranged from 0.07 to 4 nm^{-1}, where $q = 4\pi/\lambda \sin(\theta/2)$ with θ being the scattering angle. All the scattering intensity profiles were corrected for the scatterings from air and an empty cell.

4.8 Measurements of electric conductivity

ITO-deposited glass substrate patterned as shown in Figure 5a was employed for the measurement. The length of the electrode was 10 mm and the gap between electrodes was 100 μm. A solution of the polymer (10 mg) dissolved in 1 mL of chloroform was cast on the patterned substrate. The film thickness was determined by a stylus profiler as 200 nm. Measurements of conductivity at higher voltage up to 100 V were performed in a similar manner as described in our previous report on polythiophene homopolymer bearing a benzenesulfonate moiety at the side chain of thiophene.[18] The measurement perpendicular to the substrate at lower voltage (up to 10 V) was performed on a glass substrate as shown in Figure 5b, where 60 nm-thick gold electrodes with 5 nm thick chromium adhesion were deposited under a pressure of 10^{-4} to 10^{-3} Pa using a thermal evaporator with the width of 1.4 mm and the gap length between electrodes patterned as 80 μm with the thickness of 200 nm. A chloroform solution of polythiophene was cast on the substrate with the thickness of 200 nm in the glove box. The conductivity parallel to the glass substrate at lower voltage was measured with gold chromium electrode deposited on a glass substrate with the width of 1.4 nm. A polymer solution in chloroform (10 mg/1 mL) was cast with the thickness of 200 nm and a 45 nm-thick top gold electrode was deposited under a pressure of 10^{-4} to 10^{-3} Pa in the glove box using a thermal evaporator shown in Figure 5c. The current-voltage characteristics for samples of Figure 5b and 5c were measured with a semiconductor parameter analyzer in a dry-nitrogen-filled glove box at room temperature.

4.9 Measurement of electrochemical impedance spectroscopy (EIS)

The thin film electrode was prepared by spin coating. Specifically, 50 μL of copolymer solution (1 mg copolymer in 150 μL chloroform) was first drop cast on ITO glass. The solution casted ITO glass was then mounted on a spin coater where the as-prepared polymer thin-film electrode was formed under a rotation speed of 1000 rpm. The thermally treated thin film electrodes were prepared by placing the as-prepared samples into a 200 °C preheated oven for 20 minutes. To minimize contact resistance between the clamps of the potentiostat cables and the as-prepared electrode, copper tape was applied on the none-coated regions of the ITO glass to enhance the contact of aforementioned components. Finally, to prevent the interference of copper during the electrochemical measurements, a layer of epoxy resin was applied to insulate regions of the copper tape that were immersed *into* the electrolyte. A conventional three-electrode system was utilized to carry out subsequent electrochemical testing in 0.5 M $Li_2SO_{4(aq)}$ electrolyte with a Ag/AgCl reference electrode, a Pt wire counter electrode, and polymer thin-film coated ITO as the working electrode. All measurements were conducted under Ar purged conditions to prevent interference of dissolved oxygen. Electrochemical impedance spectroscopy (EIS) was performed at 0.6 V with a frequency range from 0.1 Hz to 300 kHz. Cyclic voltammetry was performed at 20 mV/s and 200 mV/s

from 0.05 V to 1.2 V vs. RHE. To avoid interference of the faradaic currents, the capacitance calculated in the range of 0.5 V to 0.95 V vs RHE. The above electrochemical techniques were performed using a Biologic SP-200 potentiostat.

Author Contributions

A. M. conceived the ideas and designed the project. S. Y. performed all of the experimental works. R. Y., C. K., and K. O. contributed synthesis and characterization of polymers. M. K. and M. F. designed measurements of electric conductivities. S.-C. Y., Y.-T. P., and M. H. designed TEM and electrochemical measurements . T. S., H. M., and H. M. supported thin-film formation and AMF measurements. All authors discussed the results and contributed to interpretation of data. A. M. wrote the manuscript with contributions from all authors.

Conflicts of interest

There are no conflicts to declare.

Acknowledgements

This work was partially supported by JSPS Kakenhi B by the MEXT (JP19182273). We thank Edanz (https://jp.edanz.com/ac) for editing a draft of this manuscript. We appreciate Professor Hsin-Lung Chen and Meng-Zhe Chen of National Tsing Hua University for valuable discussion of the morphology of polythiophene thin films and measurements of SAXS by synchrotron radiation and Professor Takashi Nishino of Kobe University for discussions on XRD measurements and thermal analyses.

References

1 H. Sirringhaus, N. Tessler and R. H. Friend, Integrated Optoelectronic Devices Based on Conjugated Polymers, *Science*, 1998, **280**, 1741–1744.

2 A. C. Grimsdale, K. Leok Chan, R. E. Martin, P. G. Jokisz and A. B. Holmes, Synthesis of Light-Emitting Conjugated Polymers for Applications in Electroluminescent Devices, *Chem. Rev.*, 2009, **109**, 897–1091.

3 P. M. Beaujuge and J. M. J. Fréchet, Molecular Design and Ordering Effects in π-Functional Materials for Transistor and Solar Cell Applications, *J. Am. Chem. Soc.*, 2011, **133**, 20009–20029.

4 I. Osaka and R. D. McCullough, Advances in Molecular Design and Synthesis of Regioregular Polythiophenes, *Acc. Chem. Res.*, 2008, **41**, 1202–1214.

5 T. Yokozawa and Y. Ohta, Transformation of Step-Growth Polymerization into Living Chain-Growth Polymerization, *Chem. Rev.*, 2016, **116**, 1950–1968.

6 T. Yokozawa and A. Yokoyama, Chain-Growth Condensation Polymerization for the Synthesis of Well-Defined Condensation Polymers and π-Conjugated Polymers, *Chem. Rev.*, 2009, **109**, 5595–5619.

7 S. Tamba, K. Shono, A. Sugie and A. Mori, C–H Functionalization Polycondensation of Chlorothiophenes in the Presence of Nickel Catalyst with Stoichiometric or Catalytically Generated Magnesium Amide, *J. Am. Chem. Soc.*, 2011, **133**, 9700–9703.

8 S. Tamba, R. Fujii, A. Mori, K. Hara and N. Koumura, Synthesis and Properties of Seleno-analog MK-organic Dye for Photovoltaic Cells Prepared by C-H Functionalization Reactions of Selenophene Derivatives, *Chem. Lett.*, 2011, **40**, 922–924.

9 Y. Shibuya and A. Mori, Dehalogenative or Deprotonative? The Preparation Pathway to the Organometallic Monomer for Transition-Metal-Catalyzed Catalyst-Transfer-Type Polymerization of Thiophene Derivatives, *Chem. Eur. J.*, 2020, **26**, 6976–6987.

10 A. Mori, Transition Metal-catalyzed Bond-forming Reactions at the C-H Bond of Heteroaromatic Compounds, *J. Synth. Org. Chem. Jpn.*, 2011, **69**, 1202–1211.

11 A. Mori, Structure and functionality-based molecular design of azoles and thiophenes, *Bull. Chem. Soc. Jpn.*, 2020, **93**, 1200–1212.

12 M. Chayer, K. Faïd and M. Leclerc, Highly Conducting Water-Soluble Polythiophene Derivatives, *Chem. Mater.*, 1997, **9**, 2902–2905.

13 H. Goto and E. Yashima, Electron-Induced Switching of the Supramolecular Chirality of Optically Active Polythiophene Aggregates, *J. Am. Chem. Soc.*, 2002, **124**, 7943–7949.

14 X. M. Hong, J. C. Tyson and D. M. Collard, Controlling the Macromolecular Architecture of Poly(3-alkylthiophene)s by Alternating Alkyl and Fluoroalkyl Substituents, *Macromolecules*, 2000, **33**, 3502–3504.

15 K. Fujita, Y. Sumino, K. Ide, S. Tamba, K. Shono, J. Shen, T. Nishino, A. Mori and T. Yasuda, Synthesis of Poly(3-substituted thiophene)s of Remarkably High Solubility in Hydrocarbon via Nickel-Catalyzed Deprotonative Cross-Coupling Polycondensation, *Macromolecules*, 2016, **49**, 1259–1269.

16 A. Mori, K. Fujita, C. Kubota, T. Suzuki, K. Okano, T. Matsumoto, T. Nishino and M. Horie, Formal preparation of regioregular and alternating thiophene–thiophene copolymers bearing different substituents, *Beilstein J. Org. Chem.*, 2020, **16**, 317–324.

17 S. Berson, S. Cecioni, M. Billon, Y. Kervella, R. de Bettignies, S. Bailly and S. Guillerez, Effect of carbonitrile and hexyloxy substituents on alternated copolymer of polythiophene-Performances in photovoltaic cells, *Sol. Energy Mater. Sol. Cells*, 2010, **94**, 699–708.

18 A. Mori, C. Kubota, K. Fujita, M. Hayashi, T. Ogura, T. Suzuki, K. Okano, M. Funahashi and M. Horie, Thermally Induced Self-Doping of π-Conjugated Polymers Bearing a Pendant Neopentyl Sulfonate Group, *Macromolecules*, 2020, **53**, 1171–1179.

19 V. Hirschberg, L. Faust, D. Rodrigue and M. Wilhelm, Effect of Topology and Molecular Properties on the Rheology and Fatigue Behavior of Solid Polystyrene/Polyisoprene Di- And Triblock Copolymers, *Macromolecules*, 2020, **53**, 5572–5587.

20 X. Yu, K. Xiao, J. Chen, N. V. Lavrik, K. Hong, B. G. Sumpter and D. B. Geohegan, High-performance field-effect transistors based on polystyrene-*b*-poly(3- hexylthiophene) diblock copolymers, *ACS Nano*, 2011, **5**, 3559–3567.

21 Y. Tian, K. Watanabe, X. Kong, J. Abe and T. Iyoda, Synthesis, Nanostructures, and Functionality of Amphiphilic Liquid Crystalline Block Copolymers with Azobenzene Moieties, *Macromolecules*, 2002, **35**, 3739–3747.

22 M. Komura and T. Iyoda, AFM Cross-Sectional Imaging of Perpendicularly Oriented Nanocylinder Structures of Microphase-Separated Block Copolymer Films by Crystal-like Cleavage, *Macromolecules*, 2007, **40**, 4106–4108.

23 A. Mori, J. Shikuma, M. Kinoshita, T. Ikeda, M. Misaki, Y. Ueda, M. Komura, S. Asaoka and T. Iyoda, Controlled Homeotropic and Homogeneous Orientations for Nanoscale Phase-separated Domain of Light-emitting Amphiphilic Block Copolymer Bearing a 2,5-Diarylthiazole Moiety, *Chem. Lett.*, 2008, **37**, 272–273.

24 Y. Takeoka, Y. Iguchi, M. Rikukawa and K. Sanui, Self-assembled multilayer films based on functionalized poly(thiophene)s, *Synth. Met.*, 2005, **154**, 109–112.

25 K. Umezawa, T. Oshima, M. Yoshizawa-Fujita, Y. Takeoka and M. Rikukawa, Synthesis of Hydrophilic–Hydrophobic Block Copolymer Ionomers Based on Polyphenylenes, *ACS Macro Lett.*, 2012, **1**, 969–972.

26 H.-R. Tseng, H. Phan, C. Luo, M. Wang, L. A. Perez, S. N. Patel, L. Ying, E. J. Kramer, T.-Q. Nguyen, G. C. Bazan and A. J. Heeger, High-Mobility Field-Effect Transistors Fabricated with Macroscopic Aligned Semiconducting Polymers, *Adv. Mater.*, 2014, **26**, 2993–2998.

27 Y. Nagao and J. Matsui, Anisotropic Proton Conductivity of Poly(aspartic acid) Thin Films, *Mater. Today Proc.*, 2019, **17**, 953–958.

28 X. M. Hong and D. M. Collard, Liquid Crystalline Regioregular Semifluoroalkyl-Substituted Polythiophenes, *Macromolecules*, 2000, **33**, 6916–6917.

29 A. Mori, C. Kubota, D. Morita, K. Fujita, S. Yamamoto, T. Suzuki, K. Okano, M. Funahashi and M. Horie, Thermally-Induced Doping of the Regioregular Polythiophene Bearing Alkylene Spacered Benzene sulfonate Group at the Side Chain, *Heterocycles*, 2021, **103**, 249–257.

30 Y.-H. Lee, Y.-L. Yang, W.-C. Yen, W.-F. Su and C.-A. Dai, Solution self-assembly and phase transformations of form II crystals in nanoconfined poly(3-hexyl thiophene) based rod-coil block copolymers, *Nanoscale*, 2014, **6**, 2194.

31 C.-A. Dai, W.-C. Yen, Y.-H. Lee, C.-C. Ho and W.-F. Su, Facile Synthesis of Well-Defined Block Copolymers Containing Regioregular Poly(3-hexyl thiophene) via Anionic Macroinitiation Method and Their Self-Assembly Behavior, *J. Am. Chem. Soc.*, 2007, **129**, 11036–11038.

32 Y.-H. Lee, W.-C. Yen, W.-F. Su and C.-A. Dai, Self-assembly and phase transformations of π-conjugated block copolymers that bend and twist: from rigid-rod nanowires to highly curvaceous gyroids, *Soft Matter*, 2011, **7**, 10429.

33 J. Bartuš, Electrically Conducting Thiophene Polymers, *J. Macromol. Sci. Part A - Chem.*, 1991, **28**, 917–924.

34 T. Ghosh, S. Nagasawa, N. Raveendran, V. Darshan, A. Saeki and V. C. Nair, Preferential Face-on and Edge-on Orientation of Thiophene Oligomers by Rational Molecular Design, *Chem. – An Asian J.*, 2019, **14**, 963–967.

35 S. Y. Son, T. Park and W. You, Understanding of Face-On Crystallites Transitioning to Edge-On Crystallites in Thiophene-Based Conjugated Polymers, *Chem. Mater.*, 2021, **33**, 4541–4550.

36 S. N. Patel, A. E. Javier and N. P. Balsara, Electrochemically Oxidized Electronic and Ionic Conducting Nanostructured Block Copolymers for Lithium Battery Electrodes, *ACS Nano*, 2013, **7**, 6056–6068.

37 A. H. Stoll and P. Knochel, Preparation of Fully Substituted Anilines for the Synthesis of Functionalized Indoles, *Org. Lett.*, 2008, **10**, 113–116.

38 W. A. Herrmann and C. Köcher, N-Heterocyclic Carbenes, *Angew. Chem., Int. Ed. Engl.*, 1997, **36**, 2162–2187.

39 R. Inoue, M. Yamaguchi, Y. Murakami, K. Okano and A. Mori, Revisiting of Benzophenone Ketyl Still: Use of a Sodium Dispersion for the Preparation of Anhydrous Solvents, *ACS Omega*, 2018, **3**, 12703–12706.